

See discussions, stats, and author profiles for this publication at: <https://www.researchgate.net/publication/231231862>

A Variety of 1D to 3D Metal–Organic Coordination Architectures Assembled with 1,1'-(2,2'-Oxybis(ethane-2,1-diyl))bis(1H-imidazole)

ARTICLE in CRYSTAL GROWTH & DESIGN · MARCH 2008

Impact Factor: 4.89 · DOI: 10.1021/cg7011217

CITATIONS

75

READS

35

6 AUTHORS, INCLUDING:



Feng Luo

Clemson University

281 PUBLICATIONS 5,045 CITATIONS

SEE PROFILE



Stuart R. Batten

Monash University (Australia)

311 PUBLICATIONS 14,180 CITATIONS

SEE PROFILE



Jimin Zheng

Nankai University

20 PUBLICATIONS 520 CITATIONS

SEE PROFILE

A Variety of 1D to 3D Metal–Organic Coordination Architectures Assembled with 1,1'-(2,2'-Oxybis(ethane-2,1-diyl))bis(1*H*-imidazole)

Yan Qi,[†] Yunxia Che,^{*,†} Feng Luo,[†] Stuart R. Batten,^{*} Yang Liu,[†] and Jimin Zheng^{*,†}

Department of Chemistry, Nankai University, Tianjin 300071, P. R. China, and School of Chemistry, Monash University, P.O. Box 23, Clayton, Victoria, 3800, Australia

Received November 13, 2007; Revised Manuscript Received January 23, 2008

ABSTRACT: A new long flexible ligand, L = 1,1'-(2,2'-oxybis(ethane-2,1-diyl))bis(1*H*-imidazole), has been prepared. The hydrothermal reactions of L with various metal ions (M(II) = Co, Zn, and Cd) as well as a series of aromatic polycarboxylate co-ligands yielded seven new metal–organic frameworks consisting of 1D, 2D, and 3D structures. Complexes **1–5** are constructed by SBU I (a M₂L₂ metallocycle), while complexes **6** and **7** are assembled by SBU II (left- and right-handed helical [M(L)]_n chains). In **1** and **2**, the SBUs I are bridged by 1,2-BDC (1,2-benzenedicarboxylate) and 3,5-DNP (3,5-dinitrophthalate) anions with the same coordination modes to generate 1D chains with repeated rings. **3** exhibits a typically 3-fold interpenetrated 3-connected (10,3)-b net. In **4**, the Co centers are connected by μ_3 -OH and carboxylic O atoms to form a cobalt–oxygen tetranuclear cluster. **5** represents an uncommon example of a 3,4-connected net with (8³)₂(8⁵ × 10) topology. In **6**, the SBUs II are extended by 1,4-BDC (1,4-benzenedicarboxylate) anions to afford highly undulated 2D (4, 4) layers. In **7**, the [Cd₃(1,3-BDC)₃] ladders connect to SBUs II to form a corrugated 2D network. A comparison of all complexes demonstrates that the structural characteristics of L ligand and organic counteranions simultaneously play an important role in the construction of the complexes. In addition, complexes **3** and **7** exhibit strong blue photoluminescence, and compound **4** is an antiferromagnet.

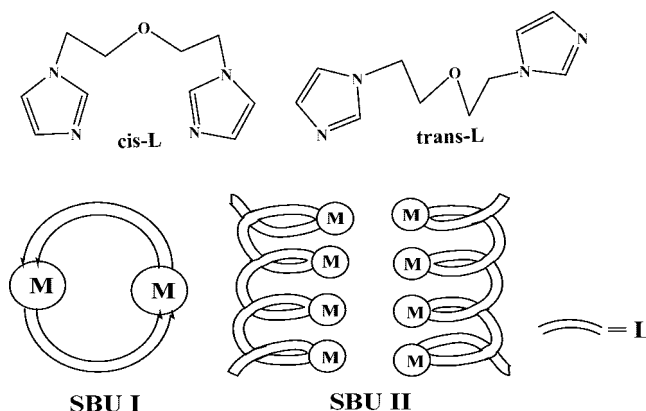
Introduction

Crystal engineering based on metal–organic frameworks (MOFs) continues to attract considerable interest, owing to their elegant framework topologies as well as their potential applications in molecular magnetism, catalysis, gas sorption, fluorescent sensing, and optoelectronic devices.¹ Studies in this field have been focused on the design and preparation, as well as the structure–property relationships. Significant progress has been achieved;² however, it is still a great challenge to rationally prepare and predict the exact structures and composition of target products built by coordination bonds and/or hydrogen bonds in crystal engineering. The resulting MOF structures are determined by several factors, including the coordination nature of metal ions, ligand structure, counterions, and so on. The design of ligands is usually a useful way of manipulating the generation of the molecular architecture.

Up to now, a large number of beautiful MOFs of ingenious design based on flexible bis(imidazole) ligands have been constructed, a series of outstanding examples of which are (N-im)₂(CH₂)_n (*n* = 1–4).^{3,4} From careful inspection of the reported cases, we found that (1) such ligands bearing alkyl spacers are a good choice of N-donor ligands, because the flexible nature of spacers allows the ligands to bend and rotate when it coordinates to metal centers, which often causes the structural diversity, and (2) the structures and properties also can be modified by changing the spacer groups, for instance, the length of the spacer.

Encouraged by all that was mentioned above, we introduced an O atom into the methylene (–CH₂–)₄ skeleton of the bis(imidazole) spacer. Thus, a new ligand, L, [1,1'-(2,2'-oxybis(ethane-2,1-diyl))bis(1*H*-imidazole)] (Scheme 1) was prepared. There are numerous advantages in the introduction of this O atom: First, the O atom increases the length of these

Scheme 1



ligands, which may control the physical dimensions of the crystalline architecture and, accordingly, affect the internal chemistry of the coordination polymers. Second, compared to 1,4-bis(imidazol-1-yl)butane (bimb), the chemical nature of the long spacer tends to favor *cis* conformation due to the orientation of C–O–C bond, which facilitates the formation of metallocyclic structures. While in the case of the previously reported coordination framework based on bimb, it is rarely reported that bimb spacers exhibit *cis* geometries.^{4a} Moreover, our newly designed N-donor ligand L hitherto has never been reported in the literature. Therefore, the exploration of this ligand is necessary to enrich and develop this field. On the other hand, multidentate O-donor organic aromatic polycarboxylate ligands, such as 1,*n*-benzenedicarboxylate (*n* = 2, 3, 4), 1,3,5-benzenetricarboxylate, and 1,2,4,5-benzenetetracarboxylate, have been extensively employed in the construction of a rich variety of high-dimensional structures, which is attributed to the diversity of the coordination modes and high structural stability.⁵ In this paper, we report our efforts in the design and synthesis of a new long flexible organic ligand, L, that combines with different aromatic polycarboxylate ligands to assemble into diverse polymeric frameworks consisting of one-, two-, or three-

* Corresponding author. Tel: +86-22-23508056. Fax: +86-22-23508056. E-mail: jmzheng@nankai.edu.cn.

[†] Nankai University.

^{*} Monash University.

dimensional structures. Seven new coordination polymers were obtained: $[\text{Co}_2(1,2\text{-BDC})_2(\text{L})_2(\text{H}_2\text{O})_2] \cdot \text{H}_2\text{O}$ (**1**), $[\text{Zn}_2(\text{DP})_2(\text{L})_2]$ (**2**), $[\text{Zn}_2(1,4\text{-BDC})_2(\text{L})_2] \cdot 3\text{H}_2\text{O}$ (**3**), $[\text{Co}_2(\text{BTC})(\mu\text{-OH})(\text{L})]$ (**4**), $[\text{Co}_4(\text{BTcC})_2(\text{L})_4] \cdot \text{H}_2\text{O}$ (**5**), $[\text{Co}(1,4\text{-BDC})(\text{L})]$ (**6**) and $[\text{Cd}_2(1,3\text{-BDC})_2(\text{L})_2]$ (**7**) ($\text{L} = [1,1'-(2,2'\text{-oxybis(ethane-2,1-diyl)})\text{bis}(1\text{H-imidazole})]$, 1,2-H₂BDC = 1,2-benzenedicarboxylic acid; 3,5-H₂DNP = 3,5-dinitrophthalic acid, 1,3-H₂BDC = 1,3-benzenedicarboxylic acid; 1,4-H₂BDC = 1,4-benzenedicarboxylic acid; H₃BTC = 1,3,5-benzenetricarboxylic acid and H₄BTcC = 1,2,4,5-benzenetetracarboxylic acid). All compounds are characterized by elemental analysis, IR spectrum and X-ray crystallography. The crystal structures as well as topological analysis of these compounds and the systematic investigation of the effect of the conformation of bis(imidazole) spacer, organic counteranions, along with different metal ions on the ultimate frameworks, will be represented and discussed. In addition, the photoluminescence properties for **3** and **7** and the magnetic properties for **4** are discussed in detail.

Experimental Section

Materials and General Procedures. Solvents and starting materials for synthesis were purchased commercially and used as received. The ligand **L** was prepared according to reported procedures.⁶ The IR spectrum was recorded as KBr pellets on a Nicolet Magna-FT-IR 560 spectrometer in the 4000–400 cm^{-1} region. Elemental analysis for C, H, and N was performed on a Perkin-Elmer 240 analyzer. The photoluminescence measurements were carried out on crystalline samples at room temperature, and the spectra were collected with a Hitachi F-2500FL spectrophotometer. The magnetic measurements were performed on the Quantum Design SQUID MPMS XL-7 instruments in a magnetic field of 1000 Oe in the temperature range of 2–300 K.

Synthesis. $[\text{Co}_2(1,2\text{-BDC})_2(\text{L})_2(\text{H}_2\text{O})_2] \cdot \text{H}_2\text{O}$ (**1**). The mixture of $\text{CoCl}_2 \cdot 6\text{H}_2\text{O}$ (0.24 g, 1.0 mmol), 1,2-H₂BDC (0.17 g, 1.0 mmol), and **L** (0.21 g, 1.0 mmol) was dissolved in 8 mL of distilled water. The pH value was then adjusted to 5.5 with 1 M NaOH solution, and the resulting mixture was transferred and sealed in a 25 mL Teflon-lined stainless steel vessel. This was then heated at 160 °C for 2 days. After the reactor was slowly cooled to room temperature, purple block-shaped crystals were filtered off, and dried in air. Yield: 42% (based on Co). Anal. Calcd for $\text{C}_{36}\text{H}_{42}\text{Co}_2\text{N}_8\text{O}_{13}$: C 47.38, H 4.64, N 12.28. Found: C 47.31, H 4.70, N 12.35. IR (KBr): $\nu(\text{cm}^{-1}) = 3480(\text{s})$, 3117(s), 3036(s), 2940(m), 1606(s), 1570(m), 1445(m), 1403(m), 1093(m), 749(m), 659(m).

$[\text{Zn}_2(\text{DNP})_2(\text{L})_2]$ (**2**). The mixture of $\text{Zn}(\text{NO}_3)_2 \cdot 6\text{H}_2\text{O}$ (0.30 g, 1.0 mmol), 3,5-H₂DNP (0.26 g, 1.0 mmol), and **L** (0.21 g, 1.0 mmol) was dissolved in 8 mL of distilled water. The pH value was then adjusted to 5.5 with 1 M NaOH solution, and the resulting mixture was transferred and sealed in a 25 mL Teflon-lined stainless steel vessel. This was then heated at 160 °C for 2 days. After the reactor was slowly cooled to room temperature, light yellow block-shaped crystals were filtered off and dried in air. Yield: 51% (based on Zn). Anal. Calcd for $\text{C}_{36}\text{H}_{32}\text{Zn}_2\text{N}_{12}\text{O}_{18}$: C 41.12, H 3.07, N 15.99. Found: C 41.17, H 3.13, N 15.93. IR (KBr): $\nu(\text{cm}^{-1}) = 3119(\text{s})$, 3053(m), 2947(m), 1611(s), 1585(m), 1522(m), 1456(m), 1405(m), 1348(m), 1103(m), 843(m), 655(m).

$[\text{Zn}_2(1,4\text{-BDC})_2(\text{L})_2] \cdot 3\text{H}_2\text{O}$ (**3**). The process was similar to **2** except that 3,5-H₂DNP was replaced by 1,4-H₂BDC (0.17 g, 1 mmol). Colorless block-shaped crystals of **3** were obtained in 45% yield (based on Zn). Anal. Calcd for $\text{C}_{36}\text{H}_{42}\text{Zn}_2\text{N}_8\text{O}_{13}$: C 46.72, H 4.57, N 12.11. Found: C 46.79, H 4.51, N 12.03. IR (KBr): $\nu(\text{cm}^{-1}) = 3415(\text{s})$, 3122(s), 3056(s), 2904(m), 1604(s), 1568(m), 1447(m), 1403(m), 1091(m), 817(m), 655(m).

$[\text{Co}_2(\text{BTC})(\mu\text{-OH})(\text{L})]$ (**4**). A purple block-shaped crystal of **4** was obtained by adopting the same synthetic procedure as **1** only using H₃BTC (0.21 g, 1.0 mmol) instead of 1,2-H₂BDC, with the pH value being adjusted to 6.0 by 1 M NaOH solution. Yield: 45% (based on Co). Anal. Calcd for $\text{C}_{19}\text{H}_{18}\text{Co}_2\text{N}_4\text{O}_8$: C 41.63, H 3.31, N 10.22. Found: C 41.58, H 3.39, N 10.25. IR (KBr): $\nu(\text{cm}^{-1}) = 3541(\text{s})$, 3154(s), 3060(s), 2952(m), 1604(s), 1572(m), 1439(m), 1408(m), 1112(m), 843(m), 708(m), 657(m).

$[\text{Co}_4(\text{BTcC})_2(\text{L})_4] \cdot \text{H}_2\text{O}$ (**5**). A purple block-shaped crystal of **5** was obtained by adopting the same synthetic procedure as **1** only using H₄BTcC (0.13 g, 0.5 mmol) instead of 1,2-H₂BDC, with the pH value being adjusted to 6.0 by 1 M NaOH solution. Yield: 38% (based on Co). Anal. Calcd for $\text{C}_{60}\text{H}_{62}\text{Co}_4\text{N}_{16}\text{O}_{21}$: C 45.64, H 3.96, N 14.19. Found: C 45.70, H 3.93, N 14.25. IR (KBr): $\nu(\text{cm}^{-1}) = 3455(\text{s})$, 3118(s), 2922(m), 1607(s), 1572(m), 1439(m), 1400(m), 1101(m), 866(m), 657(m).

$[\text{Co}(1,4\text{-BDC})(\text{L})]$ (**6**). The process was similar to **1** except that 1,2-H₂BDC was replaced by 1,4-H₂BDC (0.17 g, 1 mmol). Purple block-shaped crystals of **6** were obtained in 52% yield (based on Co). Anal. Calcd for $\text{C}_{18}\text{H}_{18}\text{CoN}_4\text{O}_5$: C 50.36, H 4.23, N 13.05. Found: C 50.44, H 4.20, N 13.09. IR (KBr): $\nu(\text{cm}^{-1}) = 3124(\text{s})$, 3040(s), 2910(m), 1586(s), 1559(m), 1469(m), 1405(m), 1089(m), 837(m), 656(m).

$[\text{Cd}_2(1,3\text{-BDC})_2(\text{L})_2]$ (**7**). The colorless block-shaped crystal of **7** was obtained by adopting the same synthetic procedure as **1** only using 1,3-H₂BDC (0.17 g, 1.0 mmol) instead of 1,2-H₂BDC and $\text{Cd}(\text{NO}_3)_2 \cdot 4\text{H}_2\text{O}$ (0.31 g, 1.0 mmol) instead of $\text{CoCl}_2 \cdot 6\text{H}_2\text{O}$. Yield: 41% (based on Cd). Anal. Calcd for $\text{C}_{36}\text{H}_{36}\text{Cd}_2\text{N}_8\text{O}_{10}$: C 44.78, H 3.76, N 11.61. Found: C 44.70, H 3.83, N 11.66. IR (KBr): $\nu(\text{cm}^{-1}) = 3112(\text{s})$, 3037(s), 2904(m), 1601(s), 1574(m), 1472(m), 1409(m), 1088(m), 862(m), 772(m), 717(m), 654(m).

X-ray Crystallographic Measurements for 1–7. Accurate unit cell parameters were determined by a least-squares fit of 2θ values, and intensity data were measured on a Rigaku θ -axis rapid IP area detector with Mo K α radiation ($\lambda = 0.71073$ Å) at room temperature. The intensities were corrected for Lorentz and polarization effects as well as for empirical absorption based on multiscan technique. All structures were solved by direct methods and refined by full-matrix least-squares fitting on F^2 by SHELX-97. All non-hydrogen atoms were refined with anisotropic thermal parameters. Crystallographic data for the seven compounds are summarized in Table 1, and selected bond lengths and angles are listed in Table S1 (Supporting Information).

Results and Discussion

Synthesis. Because the mixing of metal salt and **L** solution usually leads to precipitation, making it difficult to grow crystals of complexes, a hydrothermal technique was adopted, and seven new coordination networks were synthesized successfully. For the seven complexes, although their synthesis conditions are similar, the different geometric needs of the metal ions, the different aromatic polycarboxylate ligands, and versatile conformations of the **L** ligand have an important influence on the final crystal architectures; each one of these compounds has unique structural features.

Construction of the MOFs. Generally speaking, high-dimensional MOFs can be generated from low-dimensional building blocks by the linkage of organic ligands through metal-to-ligand bonds. The related concept, proposed by Yaghi,⁷ of the secondary building unit (SBU) has proven to be useful in understanding the construction of a given structure.⁸ In this paper, a M_2L_2 metallocycle is defined as SBU I, while $[\text{M}(\text{L})]_n$ helical polymeric chains are designated as SBU II. SBU II may be formed by the ring-opening polymerization of SBU I,⁸ as shown in Scheme 1. Combined with a series of aromatic polycarboxylate anions, SBU I and SBU II might serve as building blocks, resulting in diverse frameworks for complexes 1–7.

1D to 3D Frameworks Based on SBU I. Five polymeric structures from 1D to 3D based on SBU I are exemplified by the complexes 1–5, although the SBU I in complex **4** is defined only if two independent Co atoms are considered as a single node.

$[\text{Co}_2(1,2\text{-BDC})_2(\text{L})_2(\text{H}_2\text{O})_2] \cdot \text{H}_2\text{O}$ (**1**). Single-crystal X-ray structural analysis reveals that **1** consists of a 1D chain polymer with a M_2L_2 metallocyclic motif. The asymmetric unit of **1** consists of one independent Co(II) cation, one independent **L** molecule, one independent 1,2-BDC anion, one independent

Table 1. Crystallographic Data and Structure Refinement Details for 1–7

| | 1 | 2 | 3 | 4 |
|--|---|---|--|---|
| formula | C ₃₆ H ₄₂ Co ₂ N ₈ O ₁₃ | C ₃₆ H ₃₂ Zn ₂ N ₁₂ O ₁₈ | C ₃₆ H ₄₂ Zn ₂ N ₈ O ₁₃ | C ₁₉ H ₁₈ Co ₂ N ₄ O ₈ |
| fw | 912.63 | 1051.48 | 925.52 | 548.23 |
| T/K | 293(2) | 293(2) | 293(2) | 293(2) |
| cryst syst | monoclinic | triclinic | monoclinic | triclinic |
| space group | <i>P</i> 2 ₁ / <i>n</i> | <i>P</i> $\bar{1}$ | <i>C</i> 2/ <i>c</i> | <i>P</i> $\bar{1}$ |
| <i>a</i> /Å | 12.460(3) | 9.4863(19) | 17.935(3) | 10.650(2) |
| <i>b</i> /Å | 15.047(3) | 10.932(2) | 11.1424(17) | 10.969(2) |
| <i>c</i> /Å | 12.597(3) | 11.247(2) | 21.448(3) | 11.246(2) |
| α /deg | 90 | 100.51(3) | 90 | 111.27(3) |
| β /deg | 92.04(3) | 101.15(3) | 99.335(3) | 95.99(3) |
| γ /deg | 90 | 112.01(3) | 90 | 117.55(3) |
| <i>V</i> /Å ³ | 2360.2(8) | 1018.4(3) | 4229.4(11) | 1024.8(4) |
| <i>Z</i> | 2 | 1 | 4 | 2 |
| <i>D</i> /g/cm ³ | 1.284 | 1.714 | 1.454 | 1.777 |
| <i>F</i> (000) | 944 | 536 | 1912 | 556 |
| no. of reflns collected/unique | 22 229/5282 | 10 05/4628 | 11 909/4336 | 10 197/4655 |
| | [<i>R</i> (int) = 0.0316] | [<i>R</i> (int) = 0.0465] | [<i>R</i> (int) = 0.0428] | [<i>R</i> (int) = 0.0593] |
| GOF | 1.302 | 1.082 | 1.015 | 1.021 |
| <i>R</i> 1 [<i>I</i> > 2 σ (<i>I</i>)] | 0.0960 | 0.0699 | 0.0524 | 0.0456 |
| <i>wR</i> 2 | 0.3121 | 0.2027 | 0.1384 | 0.0905 |
| | 5 | 6 | 7 | |
| formula | C ₆₀ H ₆₂ Co ₄ N ₁₆ O ₂₁ | C ₁₈ H ₁₈ CoN ₄ O ₅ | C ₃₆ H ₃₆ Cd ₂ N ₈ O ₁₀ | |
| fw | 1578.98 | 429.29 | 965.53 | |
| T/K | 293(2) | 293(2) | 293(2) | |
| cryst syst | monoclinic | monoclinic | triclinic | |
| space group | <i>P</i> 2 ₁ / <i>c</i> | <i>C</i> 2/ <i>c</i> | <i>P</i> $\bar{1}$ | |
| <i>a</i> /Å | 18.281(4) | 7.0214(14) | 8.5363(17) | |
| <i>b</i> /Å | 13.951(3) | 19.292(4) | 10.273(2) | |
| <i>c</i> /Å | 13.260(3) | 13.871(3) | 10.811(2) | |
| α /deg | 90 | 90 | 98.53(3) | |
| β /deg | 102.23(3) | 94.98(3) | 100.10(3) | |
| γ /deg | 90 | 90 | 94.88(3) | |
| <i>V</i> /Å ³ | 3305.1(13) | 1871.8(7) | 917.0(3) | |
| <i>Z</i> | 2 | 4 | 1 | |
| <i>D</i> /g/cm ³ | 1.587 | 1.523 | 1.748 | |
| <i>F</i> (000) | 1620 | 884 | 484 | |
| no. of reflns collected/unique | 28 036/7305 | 9160/2148 | 9098/4161 | |
| | [<i>R</i> (int) = 0.1772] | [<i>R</i> (int) = 0.0300] | [<i>R</i> (int) = 0.0350] | |
| GOF | 0.909 | 1.072 | 1.190 | |
| <i>R</i> 1 [<i>I</i> > 2 σ (<i>I</i>)] | 0.0887 | 0.0281 | 0.0238 | |
| <i>wR</i> 2 | 0.1958 | 0.0705 | 0.0657 | |

coordination water, and half an independent free water molecule, as shown in Figure 1a. The Co(II) ions exhibit an irregular five-coordinated environment with two carboxylic O atoms from two 1,2-BDC anions (Co–O = 2.364(5) and 2.457(2) Å), two N atoms from two L ligands (Co–N = 2.256(6) and 2.273(6) Å), and one water molecule (Co–O = 2.375(6) Å). The longer Co–O bond indicates that the bond is weak, while the Co–N bond lengths are all within the normal range generally found in the literature.⁹ The L ligand adopts a *cis* configuration with the planes of the two imidazole rings inclined by 87.25°. Two Co(II) atoms are linked by two L ligands to form a 24-membered M₂L₂ metallocyclic ring, which is considered as SBU I, and by two 1,2-BDC anions to form 14-membered M₂BDC₂ metallocyclic rings. Each 1,2-BDC anion shows a η^1 -bridging coordination mode (Scheme 2a).¹⁰ Both types of rings are linked alternately to form an infinite 1D chain structure along the *b* axis direction (Figure 1b). Interestingly, these two kinds of rings are arranged almost perpendicular to each other. The Co...Co separations across the L ligand and 1,2-BDC anion are 9.807 and 5.254 Å, respectively. The packing of the adjacent 1D chain polymers (Figure 1c) shows significant interdigitation.

[Zn₂(DNP)₂(L)₂] (2). The key feature of the X-ray structure of **2** is similar to that of **1**, consisting of a coordination framework constructed from SBU I. There is one exception with respect to **1**: the *cis*-L is replaced by *trans*-L. The asymmetry unit of **2** consists of one independent Zn(II) ion, one independent L molecule, and one independent DNP anion. The immediate

coordination environment around the zinc center is shown in Figure 2a. Each Zn(II) center exhibits a tetrahedral coordination geometry, with two carboxylic O atoms from two DP anions (Zn–O = 1.957(3) and 1.957(4) Å) and two N atoms from two L ligands (Zn–N = 2.004(5) Å). The Zn–O/N bond lengths are all consistent with corresponding bond lengths found in the literature.¹¹ In contrast to **1**, the L ligands adopt a *trans* configuration, with dihedral angles between two imidazole rings being 72.59°, and connect two adjacent Zn atoms to generate a 24-membered M₂L₂ metallocyclic ring (SBU I) with the Zn...Zn separation being 7.749 Å. The DNP anions coordinate to the Zn atoms in the same mode as the 1,2-BDC anions in **1** (Scheme 2b) to form 14-membered metallocyclic rings with Zn...Zn separations of 5.327 Å. On the basis of the similar coordination modes to those in **1**, the chain in **2** is almost identical to that of **1**, as shown in Figure 2b. There are small differences, mainly arising from the different conformation of the L ligand.

[Zn₂(1,4-BDC)₂(L)₂]·3H₂O (3). The M₂L₂ SBU I constructed by two L ligands and two Zn(II) atoms is also observed in **3**, but this time another organic acid, 1,4-H₂BDC, was introduced, which results in a new 3D network. The asymmetric unit of **3** consists of one independent Zn(II) ion, one independent L molecule, one independent 1,4-BDC anion, and one and a half independent free water molecules (in which the O6 atom is disordered into two positions with a site occupation factor of 0.498 and 0.502, respectively). As shown in Figure 3a, the Zn(II)

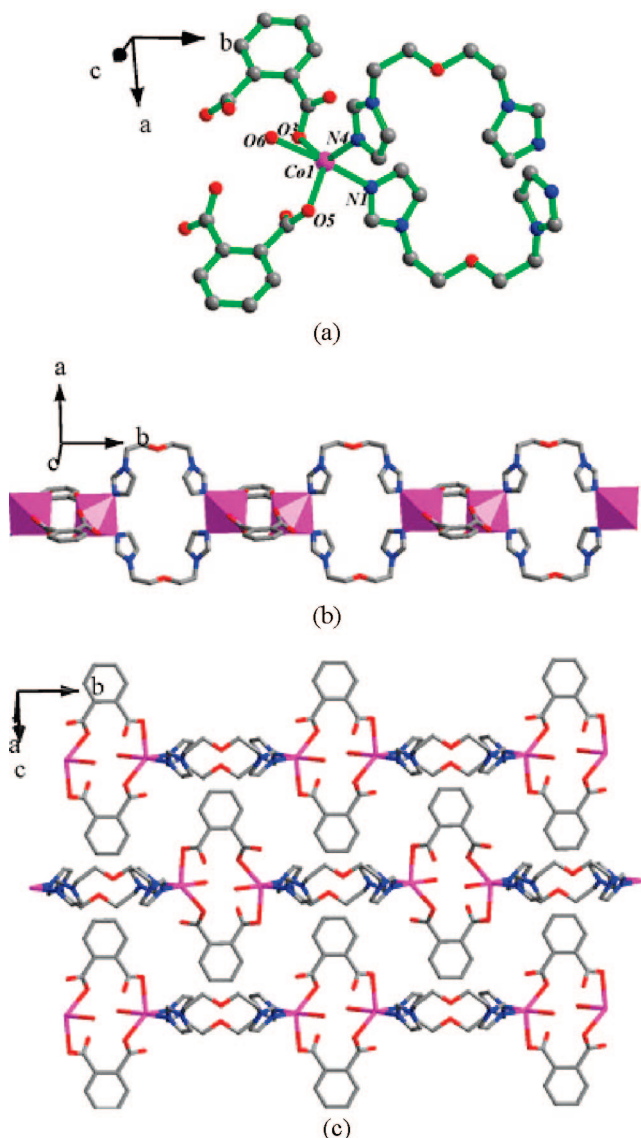


Figure 1. (a) Immediate coordination environment around the Co(II) center in **1** (the free water molecule is omitted for clarity). (b) 1D chain with repeated rings (two kinds of rings are perpendicular to each other). (c) Packing of the 1D polymers (neighboring chains are interdigitated).

ions exhibit a tetrahedral geometry with two carboxylic O atoms from two 1,4-BDC anions ($\text{Zn}-\text{O} = 1.945(3)$ and $1.926(3)$ Å) and two N atoms from two L ligands ($\text{Zn}-\text{N} = 1.990(4)$ and $2.008(4)$ Å). The Zn–O/N bond lengths are all comparable to those in **2**. The L ligand adopts a *cis* configuration with the planes of the two imidazole rings inclined by 29.32° , and the $\text{Zn}\cdots\text{Zn}$ separation across the L ligand is 6.792 Å. Two L ligands connect with two Zn(II) atoms to generate SBU I. Each 1,4-BDC anion coordinates to two Zn atoms in the same mode as those in **1** and **2** (Scheme 2c). The extension of the structure into a 3D network is accomplished by linear 1,4-BDC anions linking the SBUs I. A diamondoid network is generated¹² if the nodes are defined as being SBUs I. Water molecules are found in the adamantane cages of the network. The distances between Zn^{II} centers are 10.968 and 11.109 Å. Figure 3b shows a single cage delimited by four cyclohexane-like windows in chair conformations.

However, an alternative, perhaps better topological analysis treats the *metal centers* as the nodes. In this analysis, each metal

is connected to three others: two via single 1,4-BDC bridges and a third by pairs of L ligands. In this analysis the 4-connecting SBU I nodes are converted into a pair of linked 3-connecting nodes. The topology that results is the well-known 3-connected (10,3)-b net (Figure 3c).¹³ Moreover, the occurrence of 3-fold interpenetration in compound **3** is observed (Figure 3d).

[Co₂(BTC)(μ -OH)(L)] (4). When 1,2-BDC anions are replaced by BTC anions, a new 2D network with a tetranuclear cobalt–oxygen cluster is achieved, as shown in Figure 4a. The asymmetric unit of **4** consists of two independent Co(II) units [Co(1) and Co(2)], one independent BTC anion, one independent hydroxyl group, and one independent L. Each Co(1) is five-coordinated by three O atoms from three BTC anions ($\text{Co(1)}-\text{O} = 2.000(2)$ – $2.187(3)$ Å) and one μ_3 -OH ($\text{Co(1)}-\text{O} = 1.979(2)$ Å) and one N atom from the L ligand ($\text{Co(1)}-\text{N} = 2.073(3)$ Å). Each Co(2) is six-coordinated by three O atoms from three BTC anions ($\text{Co(2)}-\text{O} = 2.080(2)$ – $2.174(2)$ Å) and two μ_3 -OH ($\text{Co(2)}-\text{O} = 2.112(2)$ Å) and one N atom from the L ligand ($\text{Co(2)}-\text{N} = 2.112(3)$ Å). The Co(II) centers are connected by carboxylic O atoms and μ_3 -OH to form a tetranuclear cobalt–oxygen cluster (Figure 4b), which has been observed in the literature.^{4b,14} The $\text{Co}\cdots\text{Co}$ distances in the cluster are 3.087 and 3.269 Å.

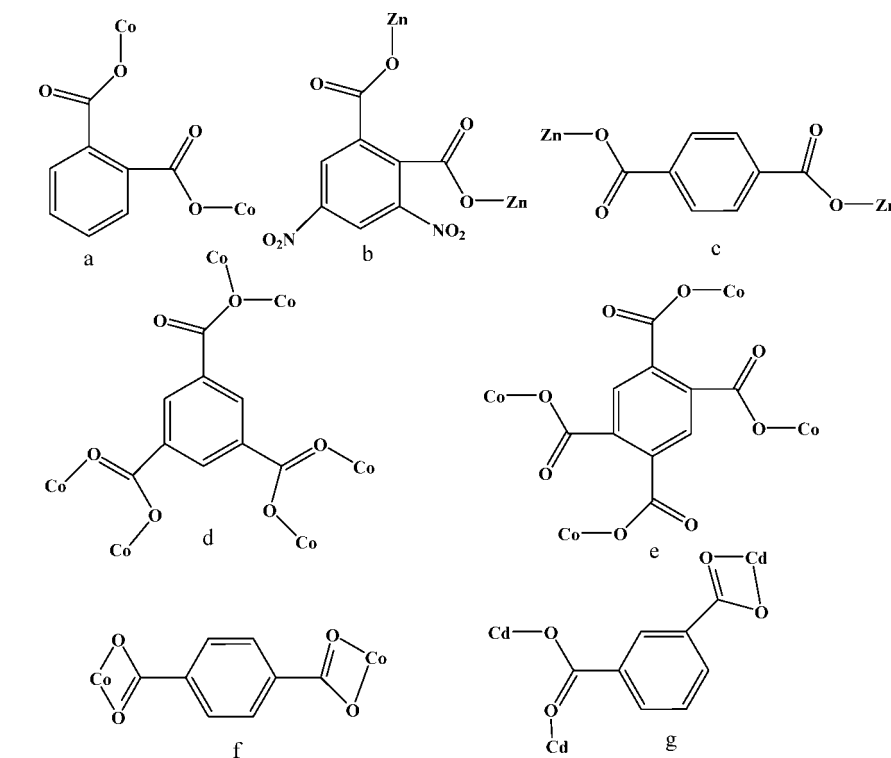
Each L ligand in **4** adopts a *cis* configuration with two imidazole rings twisted by 41.67° . If two independent Co atoms are considered as one node, SBU I is achieved by two L ligands and two such M ion dimers (Figure 4c). Each BTC anion displays a μ_6 coordination mode,^{4b} as shown in Scheme 2d, and the cobalt–oxygen clusters are connected through these BTC anions into a 2D network (Figure 4d). The 2D layer is decorated by the SBUs I on both sides (Figure 4e).

[Co₄(BTeC)₂(L)₄]·H₂O (5). When another polycarboxylate ligand, BTeC anion, was introduced, compound **5** was obtained, which exhibits a new 3D network based on the M_2L_2 metallocyclic SBU I. As shown in Figure 5a, two crystallographically independent Co(II) atoms adopt identical coordination modes. Both Co(II) atoms lie in distorted tetrahedral environments, defined by two carboxylic O atoms from two BTeC anions ($\text{Co}-\text{O} = 1.964(4)$ – $2.008(4)$ Å) and two N atoms from two L ligands ($\text{Co}-\text{N} = 1.989(6)$ – $2.019(5)$ Å). Two kinds of L ligands both adopt *cis* conformations with two imidazole rings twisted by 71.34° and 74.04° . Furthermore, two Co1 atoms are linked by two L ligands to achieve a 24-membered M_2L_2 metallocyclic SBU I ring (A), while two Co2 and two other L ligands construct another one (B). Each BTeC anion coordinates to four Co atoms (Scheme 2e) to generate a 2D layer structure (Figure 5b). Cross-linkage of the two different SBU I rings and the 2D M/BTeC layer structure results in a complicated 3D network (Figure 5c). In addition, the free water molecule forms a hydrogen bond with the coordinated carboxylic oxygen atom, with a $\text{O}\cdots\text{O}$ separation of 3.008 Å (Table S2, Supporting Information), to further stabilize the final structure.

Topological analysis of this compound reveals that it is a 3,4-connected net with $(8^3)_2(8^5 \times 10)$ topology, where the metal centers and BTeC ligands act as 3- and 4-connected nodes, respectively. Compared to known 3,4-connected nets such as boracite, Pt_3O_4 , and cubic C_3N_4 ,¹⁵ the topology of **5** is complicated, as the 3- and 4-connected nodes are not alternating linked (i.e., there are direct connections between 4-connecting nodes, Figure 5d). Therefore, it represents an uncommon example of a 3,4-connected net.

2D Networks Based on SBU II. Complexes **6** and **7** are different from those described earlier, in that they are based on

Scheme 2. Coordination Modes of Aromatic Polycarboxylate Anions



$[M(L)]_n$ helical polymeric chains. The $[M(L)]_n$ helical polymeric chain, designated as SBU II, can be formed by the ring-opening polymerization of the M_2L_2 rings (SBU I).^{8b}

[Co(1,4-BDC)(L)] (6). Single-crystal X-ray structural analysis of **6** showed that each Co(II) atom exhibits a distorted octahedral environment, composed of four carboxylic O atoms from two 1,4-BDC anions (Co–O = 2.1217(13) and 2.2080(12) Å) and two N atoms from two L ligands (Co–N = 2.0746(15) Å), as shown in Figure 6a. The L ligand adopts a *cis* configuration with two imidazole rings twisted by 54.02° and gives a Co···Co separation of 7.021 Å. Different from the structures mentioned

earlier, only one L ligand connects two adjacent Co atoms. Co atoms are arranged in left- and right-handed helices (SBUs II) as a racemate running along the *a* axis direction (Figure 6b) instead of 24-membered M_2L_2 metallocycles. Each 1,4-BDC anion coordinates to two Co atoms in the $\mu_2\text{-}\eta^3$ -chelation mode (Scheme 2f),¹⁰ which is different from that in **3**. Thus, the 1,4-BDC anions bridge two adjacent left- and right-handed helical building units to afford highly undulated 2D (4,4) layers that contain 42-membered rings with metal ions at each corner and a molecule L and a 1,4-BDC anion at each edge, respectively (Figure 6c). The lengths of the opposite edges are equal, with the distances being 10.779 and 7.021 Å, respectively, and the diagonal distances are 15.989 and 8.680 Å. The (4,4) networks of **6** stack in a parallel fashion. Perhaps surprisingly, no interpenetration occurs.

[Cd₂(1,3-BDC)₂(L)₂] (7). The introduction of 1,3-BDC results in the formation of a corrugated 2D layer in **7**, which is significantly different from **6**. As illustrated in Figure 7a, each Cd(II) atom exhibits a distorted octahedral environment with four carboxylic O atoms from three 1,3-BDC anions (Cd–O = 2.261(2)–2.5117(18) Å) and two N atoms from two L ligands (Cd–N = 2.268(2) and 2.276(2) Å). The L ligand adopts a *trans* configuration, with the planes of the two imidazole rings inclined by 43.67° to each other and the Cd···Cd separation across the L ligand being 12.545 Å. Similar to **6**, each L ligand links two adjacent Cd atoms to generate left- and right-handed helical chains (SBUs II) in pairs, as shown in Figure 7b. Each 1,3-BDC anion is connected to three Cd(II) atoms (Scheme 2g), and as shown in Figure 7c, three Cd(II) atoms are bridged by three 1,3-BDC anions to form eight-membered rings A and 16-membered rings B. These rings are arranged alternately to result in a 1D ladder-like structure. The $[Cd_3(1,3-BDC)_3]$ ladders are extended by those left- and right-handed helical chains to form a corrugated 2D network (Figure 7d), which is different from those in **6**. Such differences may mainly be attributed to the different dicarboxylate anions.

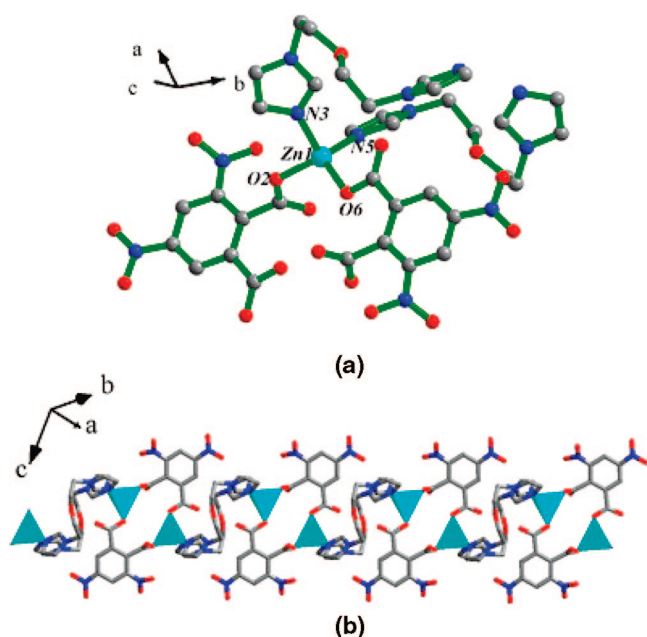


Figure 2. (a) Immediate coordination environment around the Zn(II) center in **2**. (b) 1D chain with repeated rings based on SBU I.

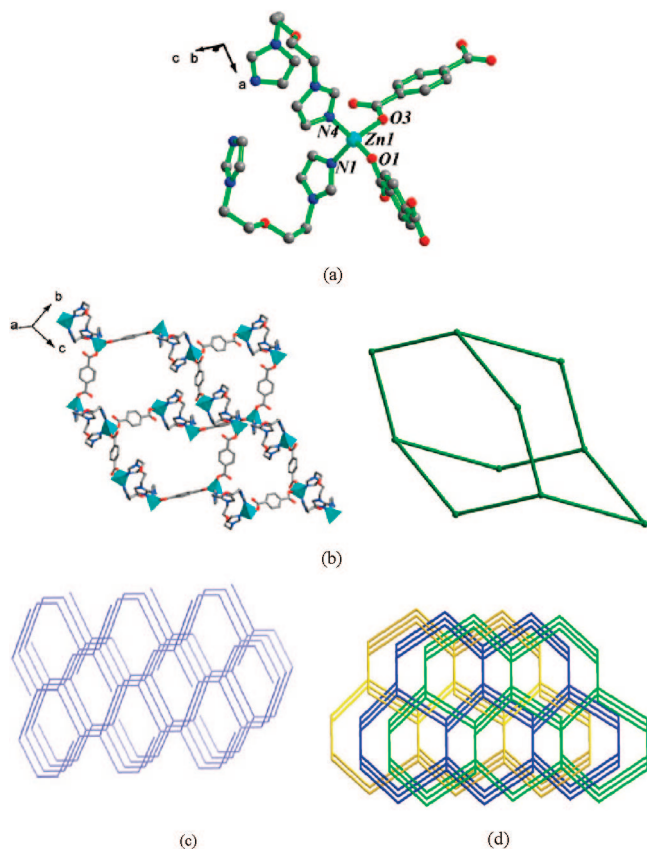


Figure 3. (a) Immediate coordination environment around the Zn(II) center in **3** (the free water molecule is omitted for clarity). (b) View of the single adamantanoid cage (left) and a schematic adamantane unit in which every node represents a SBU I (right). (c) Schematic description of the 3-connected (10,3)-b net (in this net metal atoms are the nodes). (d) Schematic description of the 3-fold interpenetrating (10,3)-b net.

Coordination Mode of L Ligand. Through comparison of the structures of **1–7**, it is apparent that the steric geometry of the flexible L ligand has a significant influence on the formation of the resulting structure. The L ligand can adopt numerous conformations, but mainly *cis* and *trans* as shown in Scheme 1, and two different metal–L motifs are formed (SBU I and SBU II). The *cis* configuration tends to generate M_2L_2 metal-locyclic structures, as found in complexes **1–5** (although in **4** the individual metal atoms are replaced by pairs of metal atoms). On the other hand, a twist of the two imidazole rings relative to the $N-(CH_2)_2-O-(CH_2)_2-N$ chain can lead to helical chains, as found in complexes **6** and **7**.

Role of the Aromatic Polycarboxylate Anions. In this study, complexes **1–7** display a variety of 1D, 2D, and 3D frameworks, and the connectivities of the seven compounds are strongly related to the aromatic polycarboxylate anions. The ratios of the metal ions and polycarboxylate anions are determined by the negative charges of the anions. Thus, the ratio is 1:1 for **1**, **2**, **3**, **6**, and **7**. The ratio of Co:BTC is 2:1 for **4**, which is attributed to the participation of two (μ -OH) units. As expected, the ratio of Co:BTcC is 2:1 for **5**. Furthermore, the versatile aromatic polycarboxylate anions show a variety of coordination modes. In **1** and **2**, the two *o*-phthalate anions (1,2-BDC or 3,5-DP) coordinate to two metal ions (Co^{II} or Zn^{II}) to form 14-membered metallocyclic rings and show the same coordination modes (Scheme 2a,b). The M_2L_2 metallocyclic SBUs I are bridged by these anions to generate 1D chains with repeated

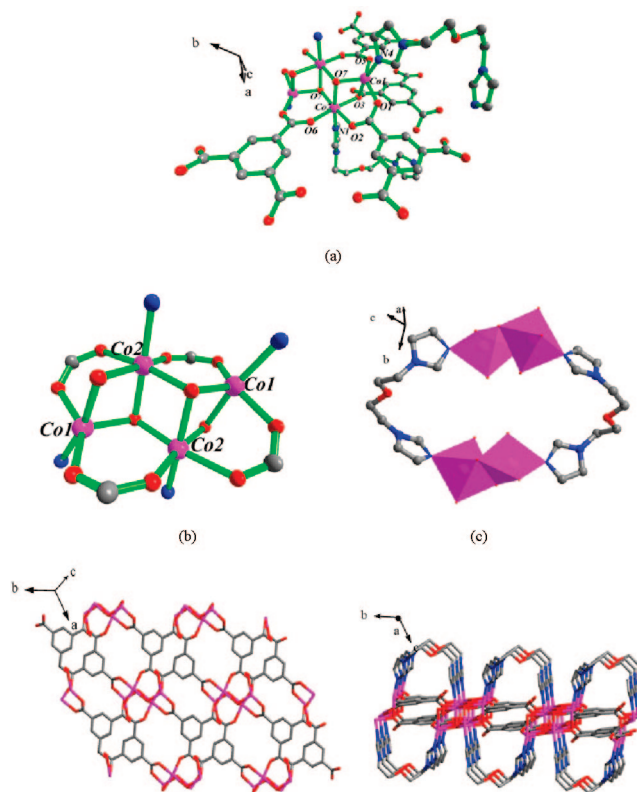


Figure 4. (a) Immediate coordination environments around the Co(II) centers in **4**. (b) Tetranuclear cobalt–oxygen cluster. (c) SBU I in complex **4**. (d) 2D layer constructed by Co(II) center and BTC anions. (e) Side view of the remarkable 2D network decorated with SBUs I on both sides.

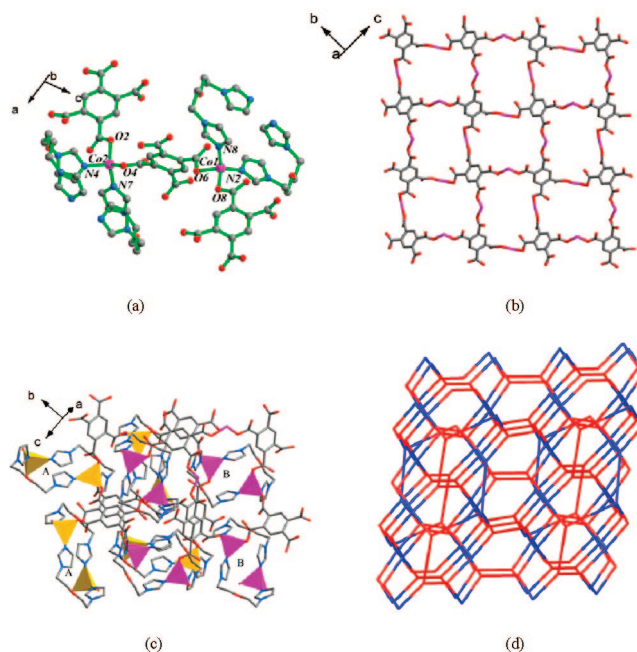


Figure 5. (a) Immediate coordination environment around the Co(II) centers in **5** (the free water molecule is omitted for clarity). (b) 2D network constructed by Co centers and BTcC anions. (c) Complicated 3D framework of **5** (rings A and B are constructed by Co1 and Co2, respectively). (d) Schematic description of the 3,4-connected net: red/3-connected metal node, blue/4-connected organic ligands.

rings. In **3** and **6**, the *p*-phthalate anions are introduced instead. Due to their different coordination modes (Scheme 2c,f), **3**

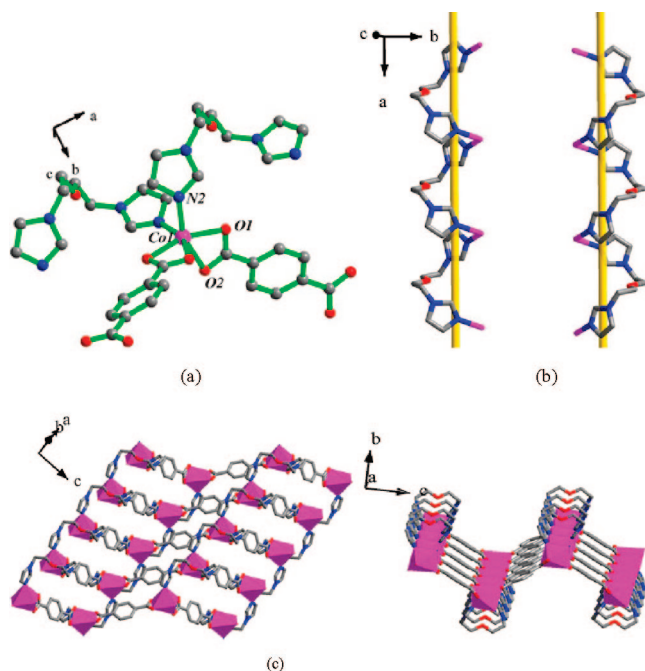


Figure 6. (a) Immediate coordination environment around the Co(II) centers in **6**. (b) 1D helical structure constructed by cobalt centers and L ligands (SBU II). (c) Front (left) and side (right) view of the highly undulated 2D (4, 4) network.

exhibits a complicated 3D framework, while **6** forms a 2D network. In **7**, each *m*-phthalate anion links three Cd(II) atoms (Scheme 2g), and the Cd centers are connected by 1,3-BDC anions to generate $[\text{Cd}_3(1,3\text{-BDC})_3]$ ladder skeletons. In **4**, each BTC anion displays a μ_6 coordination mode (Scheme 2d), and the BTC anions link the Co–O clusters to form a 2D network. In **5**, the BTeC anions each coordinate to four Co(II) ions (Scheme 2e), and the cobalt centers are connected by BTeC anions to form 2D networks. The conclusion can be easily drawn that the position and the quantity of carboxyl groups on the aromatic rings and their versatile coordination modes all have an important impact on the final frameworks.

As discussed above, the L ligands act as bidentate bridging ligands and show a tendency to form either M_2L_2 metallocycle or $[\text{M}(\text{L})_n]$ helical chain structures, no doubt determined by the orientation of the C–O–C bond. These two structural units can be considered as building blocks that are further connected by other ligands to generate high-dimension frameworks. Combination of these SBUs with a series of aromatic polycarboxylate anions that show various positions and quantities of carboxyl groups and a variety of coordination modes results in the various architectures of **1–7**. The various metal coordination geometries also play important roles in the formation of the final products. In this paper, the transition metal cations adopt various coordinated geometries, including four-, five-, and six-coordination. But it is difficult to separate and rationalize all these factors because they work together to affect the final structures, and it is thus hard to propose definitive reasons that each compound adopts a different configuration.

Photoluminescent Properties. Photoluminescent measurements of the complexes were carried out in the solid state at room temperature. The solid-state photoluminescent spectra of **3** and **7** are depicted in Figure 8. It can be seen that the intense broad photoluminescence emission at 409 nm ($\lambda_{\text{ex}} = 360$ nm) for **3** and 416 nm ($\lambda_{\text{ex}} = 318$ nm) for **7** are exhibited. The emission of **3** is assigned to an intraligand transition ($\pi-\pi^*$)

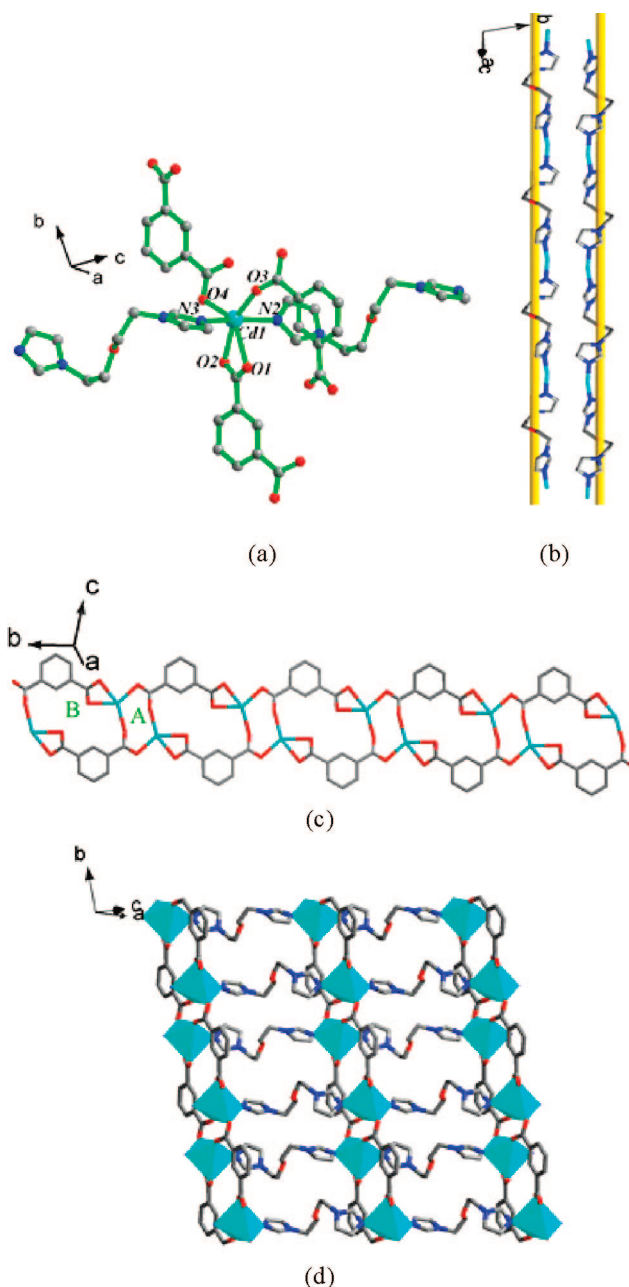


Figure 7. (a) Immediate coordination environment around the Co(II) center in **7**. (b) 1D helical structure constructed by Cd centers and L ligands (SBU II). (c) 1D $[\text{Cd}_3(1,3\text{-BDC})_3]$ ladder-like structure with rings A and B. (d) Corrugated 2D network of **7**.

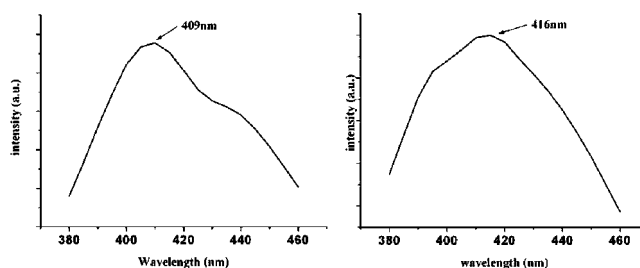


Figure 8. Solid-state emission spectra of compounds **3** (left) and **7** (right) at room temperature.

of the L ligand,^{16a} because the Zn(II) ion is difficult to oxidize or to reduce due to its d^{10} configuration.^{16b} The emission of **7**

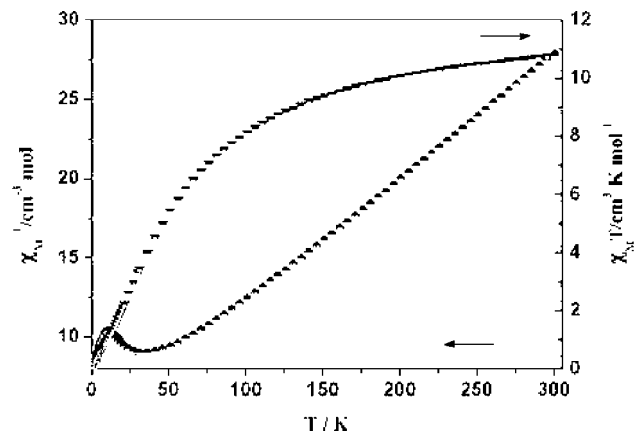


Figure 9. Plot of the temperature dependence of $\chi_M T$ (triangles) and χ_M^{-1} (nodes) for compound **4**.

may be due mainly to σ -donation from the coordination environment of the Cd(II) centers and thus be assigned as ligand-to-metal charge-transfer (LMCT).¹⁷ The emission in the blue region indicates that these complexes appear to be good candidates for promising blue-light-emitting materials. Complexes **1**, **4**, **5**, and **6** do not exhibit detectable photoluminescence; the luminescence emission may be quenched by the Co(II) ions.¹⁸ Unfortunately, the reason for no clear photoluminescence in **2** is not clear with our present state of knowledge.

Magnetic Properties. The temperature-dependent magnetic susceptibility data of compound **4** have been measured for polycrystalline samples at an applied magnetic field of 1000 Oe in the temperature range 2–300 K (Figure 9). The $\chi_M T$ value at 300 K is $10.78 \text{ cm}^3 \text{ mol}^{-1} \text{ K}$ (χ_M is the molar magnetic susceptibility for four Co(II) ions), which is far larger than the theoretic value $7.5 \text{ cm}^3 \text{ K mol}^{-1}$ for four spin-only Co(II) ions ($S = 3/2$ with $g = 2.0$).¹⁹ This may be ascribed to the unquenched orbital contribution of Co(II) ions.²⁰ Upon cooling of the sample, the values of $\chi_M T$ smoothly decrease to $5.43 \text{ cm}^3 \text{ mol}^{-1} \text{ K}$ around 50 K, then sharply decrease to $0.25 \text{ cm}^3 \text{ mol}^{-1} \text{ K}$ at 2.0 K. The magnetic susceptibility above 60 K can be well fit to the Curie–Weiss law with $\theta = -61.75 \text{ K}$. The negative θ value confirms the presence of antiferromagnetic interactions between Co(II) ions.

Conclusion

The simultaneous use of the new flexible bis(imidazole) ligand (L) and aromatic polycarboxylate anions to react with metal ions (Co^{II} , Zn^{II} , and Cd^{II}) affords seven interesting polymeric architectures, demonstrating again the aesthetic diversity of coordination chemistry. These seven frameworks are the first reported examples of extended coordination polymers incorporating the L ligand. The results of this study not only illustrate that the different aromatic polycarboxylate ligands and the nature of the neutral ligands play an important role in the construction of coordination polymers but also indicate that the introduction of a heteroatom into the methylene ($-\text{CH}_2-$)_n skeleton of bis(imidazole) spacers is an efficient method for construction of novel MOFs. In addition, the concept of SBU is helpful to understand the construction of a given structure. It is believed that more metal complexes containing flexible N-donor ligands and aromatic polycarboxylate anions with interesting structures as well as physical properties will be synthesized.

Acknowledgment. This work was supported by the National Natural Science Foundation of China (50572040).

Supporting Information Available: X-ray crystallographic files in CIF format, tables of bond lengths and angles for all the compounds (Table S1), and hydrogen-bonding data of complex **5** (Table S2). This material is available free of charge via the Internet at <http://pubs.acs.org>.

References

- (1) (a) Janiak, C. *Dalton Trans.* **2003**, 2781. (b) James, S. L. *Chem. Soc. Rev.*, **2003**, 32, 276. (c) Rosi, N. L.; Eckert, J.; Eddaoudi, M.; Vodak, D. T.; Kim, J.; O'Keeffe, M.; Yaghi, O. M. *Science* **2003**, 300, 1127.
- (2) (a) Yaghi, O. M.; O'Keeffe, M.; Ockwig, N. W.; Chae, H. K.; Eddaoudi, M.; Kim, J. *Nature* **2003**, 423, 705. (b) Friedrichs, O. D.; O'Keeffe, M.; Yaghi, O. M. *Acta Crystallogr.* **2003**, A59, 22. (c) Friedrichs, O. D.; O'Keeffe, M.; Yaghi, O. M. *Acta Crystallogr.* **2003**, A59, 515.
- (3) (a) Jin, C. M.; Lu, H.; Wu, L. Y.; Huang, J. *Chem. Commun.* **2006**, 5039. (b) Li, X. J.; Wang, X. Y.; Gao, S.; Cao, R. *Inorg. Chem.* **2006**, 45, 1508. (c) Li, X. J.; Cao, R.; Guo, Z. G.; Bi, W. H.; Yuan, D. Q. *Inorg. Chem. Commun.* **2006**, 9, 551. (d) Cui, G. H.; Li, J. R.; Tian, J. L.; Bu, X. H.; Batten, S. R. *Cryst. Growth Des.* **2005**, 5, 1775. (e) Wang, X. Y.; Li, B. L.; Zhu, X.; Gao, S. *Eur. J. Inorg. Chem.* **2005**, 3277.
- (4) (a) Wen, L. L.; Liu, Z. D.; Lin, J. G.; Tian, Z. F.; Zhu, H. Z.; Meng, Q. J. *Cryst. Growth Des.* **2007**, 7, 93. (b) Liu, Y. Y.; Ma, J. F.; Yang, J.; Su, Z. M. *Inorg. Chem.* **2007**, 46, 3027. (c) Li, F. F.; Ma, J. F.; Song, S. Y.; Yang, J.; Jia, H. Q.; Hu, N. H. *Cryst. Growth Des.* **2006**, 6, 209. (d) Yang, J.; Ma, J. F.; Liu, Y. Y.; Ma, J. C.; Jia, H. Q.; Hu, N. H. *Eur. J. Inorg. Chem.* **2006**, 1208. (e) Ma, J. F.; Yang, J.; Zheng, G. L.; Li, L.; Zhang, Y. M.; Li, F. F.; Liu, J. F. *Polyhedron* **2004**, 23, 553. (f) Ma, J. F.; Yang, J.; Zheng, G. L.; Li, L.; Liu, J. F. *Inorg. Chem.* **2003**, 42, 7531. (g) Ballester, L.; Baxter, I.; Duncan, P. C. M.; Goodgame, D. M. L.; Grachvogel, D. A.; Williams, D. J. *Polyhedron* **1998**, 17, 3613. (h) Goodgame, D. M. L.; Menzer, S.; Williams, D. J. *Chem. Commun.* **1996**, 2127.
- (5) For examples: (a) James, S. L. *Chem. Soc. Rev.* **2003**, 32, 276. (b) Kumagai, H.; Kepert, C. J.; Kurmoo, M. *Inorg. Chem.* **2002**, 41, 3410, and references therein. (c) Livage, C.; Guillo, N.; Marrot, J.; Ferey, G. *Chem. Mater.* **2001**, 13, 4387. (d) Kepert, C. J.; Prior, T. J.; Rosseinsky, M. J. *J. Am. Chem. Soc.* **2000**, 122, 5158. (e) Chui, S. S.-Y.; Lo, S. M.-F.; Charmant, J. P. H.; Orpen, A. G.; Williams, I. D. *Science* **1999**, 283, 1148. (f) Kepert, C. J.; Rosseinsky, M. J. *Chem. Commun.* **1998**, 31. (g) Yaghi, O. M.; Davis, C. E.; Li, G.; Li, H. *J. Am. Chem. Soc.* **1997**, 119, 2861. (h) Gutsche, G. O. H.; Molinier, M.; Powell, A. K.; Winpenny, R. E. P.; Wood, P. T. *Chem. Commun.* **1996**, 823. (i) Yaghi, O. M.; Li, H.; Groy, T. L. *J. Am. Chem. Soc.* **1996**, 118, 9096.
- (6) Schütze, W.; Schubert, H. *J. Prakt. Chem.* **1959**, 8, 306.
- (7) (a) Eddaoudi, M.; Kim, J.; Wachter, J. B.; Chae, H. K.; Keffe, M.; Yaghi, O. M. *J. Am. Chem. Soc.* **2001**, 123, 4368. (b) Vodak, D. T.; Braun, M. E.; Kim, J.; Eddaoudi, M.; Yaghi, O. M. *Chem. Commun.* **2001**, 2534. (c) Kim, J.; Chen, B.; Reineke, T. M.; Li, H.; Eddaoudi, M.; Moler, D. B.; O'Keeffe, M.; Yaghi, O. M. *J. Am. Chem. Soc.* **2001**, 123, 8239.
- (8) (a) Kurmoo, M.; Kumagai, H.; Akita-Tanaka, M.; Inoue, K.; Takagi, S. *Inorg. Chem.* **2006**, 45, 1627. (b) Zhang, L.; Lü, X. Q.; Chen, C. L.; Tan, H. Y.; Zhang, H. X.; Kang, B. S. *Cryst. Growth Des.* **2005**, 5, 283. (c) Wang, X.; Qin, C.; Wang, E.; Li, Y.; Hu, C.; Xu, L. *Chem. Commun.* **2004**, 378. (d) Dan, M.; Udayakumar, D.; Rao, C. N. R. *Chem. Commun.* **2003**, 2212. (e) Bu, X. H.; Chen, W.; Lu, S. L.; Zhang, R. H.; Liao, D. Z.; Bu, W. M.; Shionoya, M.; Brisse, F.; Ribas, J. *Angew. Chem., Int. Ed.* **2001**, 40, 3201.
- (9) (a) Chen, P. K.; Che, Y. X.; Xue, L.; Zheng, J. M. *Cryst. Growth Des.* **2006**, 6, 2517. (b) Lu, J.; Yu, C.; Niu, T.; Paliwala, T.; Crisci, G.; Somosa, F.; Jacobson, A. J. *Inorg. Chem.* **1998**, 37, 4637. (c) Jung, O. S.; Park, S. H.; Kim, K. M.; Jang, H. G. *Inorg. Chem.* **1998**, 37, 5781.
- (10) Chawla, S. K.; Arora, M.; Näntinen, K.; Rissanen, K.; Yakhmi, J. V. *Polyhedron* **2004**, 23, 3007.
- (11) (a) Tian, Z. F.; Lin, J. G.; Su, Y.; Wen, L. L.; Liu, Y. M.; Zhu, H. Z.; Meng, Q. J. *Cryst. Growth Des.* **2007**, ASAP. (b) Wang, X. L.; Qin, C.; Wang, E. B.; Su, Z. M. *Chem.-Eur. J.* **2006**, 12, 2680.
- (12) (a) Xiong, R. G.; You, X. Z.; Abrahams, B. F.; Xue, Z. L.; Che, C. M. *Angew. Chem., Int. Ed.* **2001**, 40, 4422. (b) Xiong, R. G.; Zuo, J. L.; You, X. Z.; Bai, Z. P.; Abrahams, B. F.; Che, C. M.; Fun, H. K. *Chem. Commun.* **2000**, 2061.
- (13) Batten, S. R.; Robson, R. *Angew. Chem., Int. Ed.* **1998**, 37, 1460.
- (14) (a) Fan, J.; Hanson, B. E. *Inorg. Chem.* **2005**, 44, 6998. (b) Harrison, W. T. A.; Gier, T. E.; Stucky, G. D.; Broach, R. W.; Bedard, R. A.

- Chem. Mater.* **1996**, 8, 145. (c) Liu, Y. L.; Na, L. Y.; Zhu, G. S.; Xiao, F. S.; Pang, W. Q.; Xu, R. R. *J. Solid State Chem.* **2000**, 149, 107.
- (15) (a) Luo, F.; Zheng, J. M.; Batten, S. R. *Chem. Commun.* **2007**, 3744. (b) Dybtsev, D. N.; Chun, H.; Kim, K. *Chem. Commun.* **2004**, 1594. (c) Luo, F.; Che, Y. X.; Zheng, J. M. *Inorg. Chem. Commun.*, **2006**, 9, 1045.
- (16) (a) Fun, H. K.; Raj, S. S. S.; Xiong, R. G.; Zuo, J. L.; Yu, Z.; You, X. Z. *J. Chem. Soc., Dalton Trans.* **1999**, 1915. (b) Kurtz, S. K.; Perry, T. T. *J. Appl. Phys.* **1968**, 39, 3798.
- (17) Li, X. J.; Cao, R.; Bi, W. H.; Wang, Y. Q.; Wang, Y. L.; Li, X.; Guo, Z. G. *Cryst. Growth Des.* **2005**, 5, 1651.
- (18) Zhu, H. F.; Fan, J.; Okamura, T.; Sun, W. Y.; Ueyama, N. *Cryst. Growth Des.* **2005**, 5, 289.
- (19) Ghoshal, D.; Mostafa, G.; Maji, T. K.; Zangrando, E.; Lu, T.-H.; Ribas, J.; Chaudhuri, N. R. *New J. Chem.* **2004**, 28, 1204.
- (20) (a) Boudalis, A. K.; Raptopoulou, C. P.; Abarca, B.; Ballesteros, R.; Chadlaoui, M.; Tuchagues, J. P.; Terzis, A. *Angew. Chem., Int. Ed.* **2006**, 45, 432. (b) Telfer, S. G.; Kuroda, R.; Lefebvre, J.; Leznoff, D. B. *Inorg. Chem.* **2006**, 45, 4592.

CG7011217